Using Shear Strain Localisation to Model the Fracturing Around Gallery in Unsaturated Callovo-Oxfordian Claystone

B. Pardoen, S. Levasseur and F. Collin

Abstract Galleries drilling leads to damage propagation, fracturing and properties modifications in the surrounding medium. The prediction of the damaged zone behaviour is an important matter and needs to be properly assessed. To do so the fractures can be modelled using shear strain localisation. The coupled local second gradient model is used under unsaturated conditions to correctly model the strain localisation behaviour. The permeability evolution and the rock desaturation due to air ventilation in galleries are considered. Finally, a hydro-mechanical modelling of a gallery excavation in Callovo-Oxfordian claystone is performed leading to a fairly good representation of the damaged zone.

1 Introduction

Owing to its low permeability, the Callovo-Oxfordian claystone is nowadays considered as a favorable medium for nuclear waste repository. In this rock, the gallery excavation induces damage propagation, fractures and drastic properties changes leading to the development of the excavation damaged zone (Fig. 1). The safety function of the host rock may be altered thus predicting the fracturing structure and behaviour of this zone is crucial.

Numerous experimental works have emphasize that strain localisation in shear band mode appears prior to fractures, therefore we propose to model the damaged zone by considering this mode of strain localisation. Among the existing enhanced models with regularisation methods that allow a proper modelling of the strain localisation behaviour, we use the coupled local second gradient model under unsaturated conditions. Moreover, it is known that hydraulic permeability is not homogeneous in the damaged zone (Tsang et al. 2005), then its modification is considered through a dependency with shear band properties.

B. Pardoen (✉) · S. Levasseur · F. Collin
ArGEnCo Department, University of Liège, 4000 Liège, Belgium
e-mail: b.pardoen@ulg.ac.be

K.-T. Chau and J. Zhao (eds.), *Bifurcation and Degradation of Geomaterials in the New Millennium*, Springer Series in Geomechanics and Geoengineering,
DOI 10.1007/978-3-319-13506-9_41

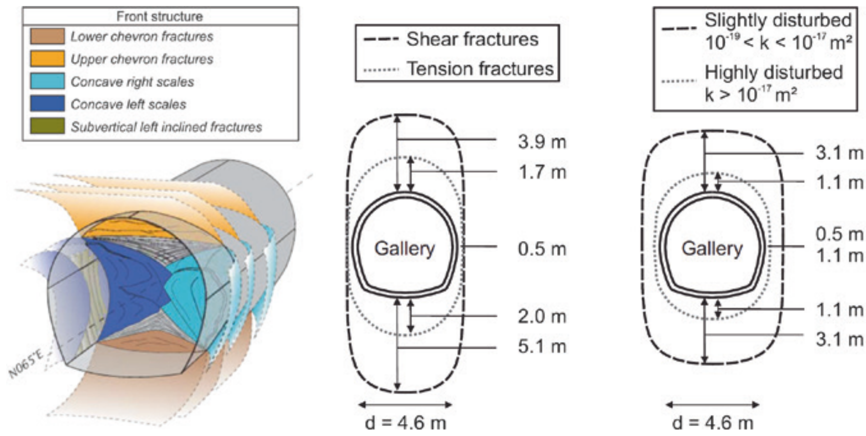

Fig. 1 In situ fractures and permeability in Callovo-Oxfordian claystone (Armand et al. 2014)

2 Coupled Local Second Gradient Model

Within the framework of classical finite elements, the strain localisation depends on the mesh size and orientation (Collin et al. 2009). An enhanced model, introducing an internal length scale, is thus needed to correctly model the post peak and localisation behaviour. Among the different regularization methods, the second gradient local model (Chambon et al. 1998) is used. In the latter, the continuum is enriched with microstructure effects: the kinematics includes the classical ones (macro) and the microkinematics (Mindlin 1964). For coupled second gradient model, the two balance equations to be solved (Collin et al. 2006), for every kinematically admissible virtual displacement field u_i^* and virtual pore water pressure field p_w^*, read in a weak form:

$$\int_{\Omega} \left(\sigma_{ij} \frac{\partial u_i^*}{\partial x_j} + \Sigma_{ijk} \frac{\partial^2 u_i^*}{\partial x_j \partial x_k} \right) d\Omega = \int_{\Gamma_\sigma} \left(\bar{t}_i u_i^* + \bar{T}_i D u_i^* \right) d\Gamma \tag{1}$$

$$\int_{\Omega} \left(\dot{M} p_w^* - m_i \frac{\partial p_w^*}{\partial x_i} \right) d\Omega = \int_{\Omega} Q p_w^* d\Omega + \int_{\Gamma_q} \bar{q} p_w^* d\Gamma \tag{2}$$

where σ_{ij} is the total stress field, Σ_{ijk} is the double stress dual of the (micro) second gradient, which needs an additional constitutive law, and Ω denotes the current solid configuration (volume). t_i is the external traction (classical) forces per unit area, T_i is an additional external (double) force per unit area, both applied on a part Γ_σ of the boundary of Ω and Du_i is u_i normal derivative. Further, M is the time derivative of the water mass inside Ω, m_i is the mass flow, Q is a sink term and Γ_q is the part of the boundary where the input water mass per unit area $\bar{q}$ is prescribed.

The total stress field is defined according to Bishop's postulate, corresponding to Biot's definition and taking into account partial saturation: $\sigma_{ij} = \sigma'_{ij} - b\, S_{r,w}\, p_w\, \delta_{ij}$ where σ'_{ij} is the effective stress, b is Biot's coefficient, $S_{r,w}$ is the water degree of saturation and δ_{ij} is the Kronecker symbol.

3 Constitutive Models

The constitutive mechanical law used for the clayey rock is an elastoplastic model with a Drucker-Prager yield surface. It includes friction angle hardening and cohesion softening as a function of the Von Mises equivalent plastic strain. The second gradient law gives Σ_{ijk} as a function of the (micro) second gradient. It is a linear elastic law with isotropic linear relationship deduced from Mindlin (1964) and it depends only on one elastic parameter D. The shear band width is proportional to this elastic parameter (Chambon et al. 1998) and Σ_{ijk} has no link with p_w.

A flow model is used to reproduce water transfer in partially saturated porous media. The advection of the liquid phase is modelled by Darcy's flow. The retention and the water relative permeability curves are given by van Genuchten's model (van Genuchten 1980). Because hydraulic properties are not homogeneous in the damaged zone, a modification of the intrinsic hydraulic permeability tensor k_{ij} is considered through a dependency with a mechanical parameter. Considering an exponential formulation depending on the porosity n (Chavant and Fernandes 2005) or on the total equivalent strain ε_{eq}:

$$k_{ij} = k_{ij,0}\left(1 + \alpha(n - n_0)^{\beta}\right) \qquad or \qquad k_{ij} = k_{ij,0}\left(1 + \alpha(\varepsilon_{eq} - \varepsilon^{t}_{eq})^{\beta}\right) \quad (3)$$

where $k_{ij,0}$ is the initial intrinsic hydraulic permeability tensor, α and β are two coefficients of the permeability evolution, n_0 is the initial porosity, ε_{eq} is the total equivalent strain $\varepsilon_{eq} = 1.5\sqrt{\hat{\varepsilon}_{ij}\hat{\varepsilon}_{ij}}$, $\hat{\varepsilon}_{ij}$ is the total deviatoric strain $\hat{\varepsilon}_{ij} = \varepsilon_{ij} - (\varepsilon_{kk}/3)\,\delta_{ij}$, ε^{t}_{eq} is a threshold value from which the permeability increases, below this value no permeability change occurs. The mechanical and hydraulic parameters for the Callovo-Oxfordian claystone are detailed in the Table 1.

4 Numerical Modelling and Results

The major issue of the simulations is the prediction of the damaged zone behaviour and fracturing structure that develops due to excavation. A hydro-mechanical modelling of a gallery excavation is performed in two-dimensional plane strain state. It takes into account the hydraulic permeability anisotropy and the initial anisotropic stress state corresponding to a gallery of the Andra URL drilled in Callovo-Oxfordian claystone and oriented in the direction of the minor horizontal principal stress. A schematic representation of the model, the mesh, the initial conditions and the boundary conditions is detailed in Fig. 2.

Table 1 Mechanical and hydraulic parameters for the Callovo-Oxfordian claystone

Parameter	Symbol	Name	Value	Unit
Mechanical	E	Young's modulus	4,000	MPa
	ν	Poisson's ratio	0.3	–
	b	Biot's coefficient	0.6	–
	ψ	Dilatancy angle	0.5	°
	φ_0	Initial friction angle	10	°
	φ_f	Final friction angle	20	°
	c_0	Initial cohesion	3	MPa
	c_f	Final cohesion	0.3	MPa
	D	Second gradient elastic modulus	5,000	N
Hydraulic	$k_{xx,0}$	Initial horizontal intrinsic water permeability	4×10^{-20}	m^2
	$k_{yy,0}$	Initial vertical intrinsic water permeability	1.33×10^{-20}	m^2
	n_0	Initial porosity	0.18	–
	M	van Genuchten coefficient	0.33	–
	N	van Genuchten coefficient	1.49	–
	P_r	van Genuchten air entry pressure	15	MPa

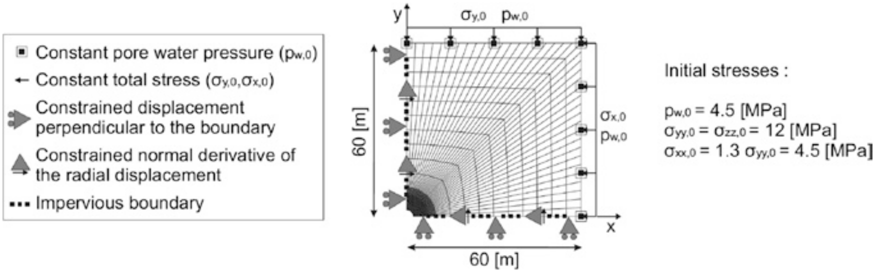

Fig. 2 Representation of the model used for the modelling of the gallery excavation

During the excavation, which lasts 5 days, the radial stresses and the pore water pressure at gallery wall decrease from their initial values to one atmospheric pressure. Then, gallery ventilation is performed. The air inside the gallery is considered to have a relative humidity of 80 %, which corresponds by Kelvin's law to a suction of $p_w = -30.7$ MPa. This constant suction is applied on the gallery wall after the excavation.

The results provide information about the damaged zone extension, structure and behaviour. A chevron fracture pattern develops during the drilling (Fig. 3) with an extension in the rock mass corresponding to in situ experimental measurements of shear fractures (Fig. 1).

Following Eq. 3, a cubic evolution of intrinsic permeability with porosity is considered ($\alpha = 2 \times 10^{12}$, $\beta = 3$). In Fig. 4, one can observe that the porosity increases close to the gallery. The horizontal intrinsic permeability evolution along the x and y-axis indicates that even if this increase is higher in the shear bands, it remains quite diffuse in the gallery vicinity because porosity is linked to volumetric strain.

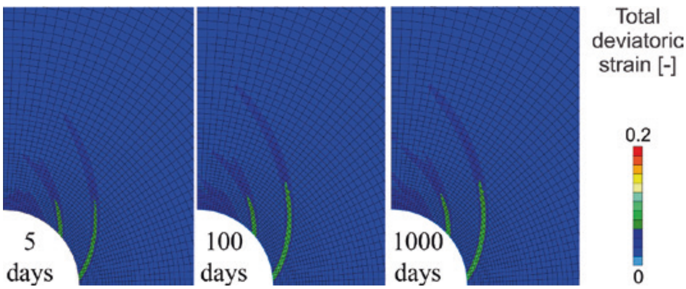

Fig. 3 Evolution of strain localisation bands pattern after the excavation

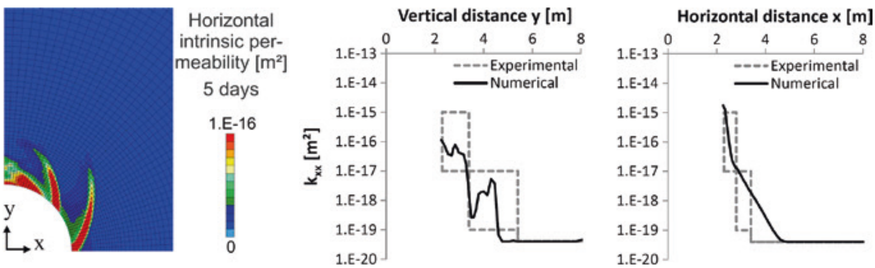

Fig. 4 Evolution of horizontal intrinsic permeability with porosity at the end of excavation (*left*) 2D view, (*middle*) vertical cross-section on y-axis, (*right*) horizontal cross section on x-axis

To better represent the permeability increase in the fractures represented by shear bands, a cubic evolution with the total equivalent strain can be considered (Eq. 3, $\alpha = 2 \times 10^8$, $\beta = 3$). In fact, this evolution only considers a dependence with the deviatoric strain, i.e. shear strain, and the threshold value $\varepsilon_{eq}^{t} = 0.01$ allows to restrict the permeability increase in the shear bands as indicates in Fig. 5. Furthermore, the in situ experimental measures of permeability are well reproduced (Figs. 1, 4 and 5). The damaged zone desaturation, due to gallery ventilation and

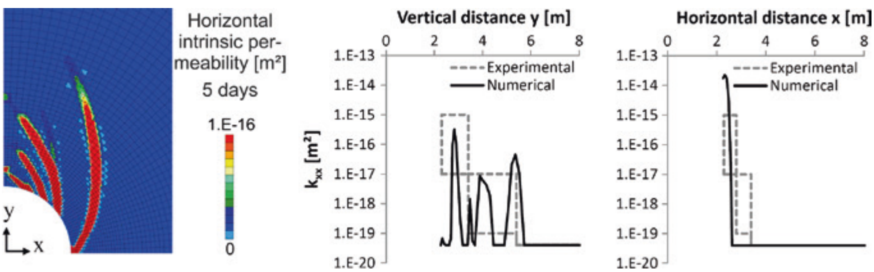

Fig. 5 Evolution of horizontal intrinsic permeability with total equivalent strain at the end of excavation (*left*) 2D view, (*middle*) vertical cross-section on y-axis, (*right*) horizontal cross section on x-axis

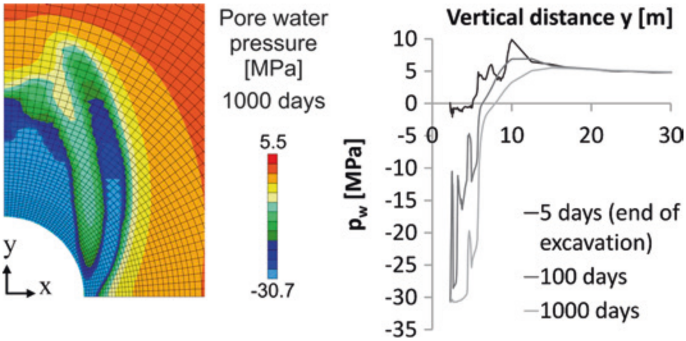

Fig. 6 Pore water pressure evolution when permeability depends on total equivalent strain (*left*) 2D view after 1,000 days of ventilation, (*right*) vertical cross-section on y-axis

rock-atmosphere interaction, is also well reproduced (Fig. 6) thanks to the permeability increase in the fractures. The results along the y-axis in Fig. 6 highlight a strong desaturation, which extends a few meters in the rock, its evolution during time and the influence of the shear strain localisation bands on the pore water pressure.

5 Conclusion

The excavation damaged zone around a gallery and its behaviour is successfully reproduced. First, the fractures are properly represented using shear strain localisation and the coupled local second gradient model. Second, the permeability increase within the fractures corresponds to in situ measurements. Finally, the rock desaturation resulting from gallery ventilation is well reproduced.

References

Armand G, Leveau F, Nussbaum C, de La Vaissiere R, Noiret A, Jaeggi D, Landrein P, Righini C (2014) Geometry and properties of the excavation-induced fractures at the Meuse/Haute-Marne URL drifts. Rock Mech Rock Eng 47(1):21–41

Chambon R, Caillerie D, Hassan NE (1998) One-dimensional localisation studied with a second grade model. Eur J Mech A-Solid 17(4):637–656

Chavant C, Fernandes R (2005) Evaluating the reliability of hydro-mechanical simulation: a benchmark of numerical techniques carried out by Research Group of MoMas. In: Second international meeting clays in natural & engineered barriers for radioactive waste confinement, Tours, 14–18 March 2005, pp 249–250

Collin F, Chambon R, Charlier R (2006) A finite element method for poro mechanical modelling of geotechnical problems using local second gradient models. Int J Numer Meth Eng 65(11):1749–1772

Collin F, Levasseur S, Chambon R (2009) Numerical post failure methods in multiphysical problems. Eur J Environ Civ Eng 13(7–8):983–1004

Mindlin RD (1964) Micro-structure in linear elasticity. Arch Ration Mech Anal 16(1):51–78
Tsang CF, Bernier F, Davies C (2005) Geohydromechanical processes in the excavation damaged zone in crystalline rock, rock salt, and indurated and plastic clays—in the context of radioactive waste disposal. Int J Rock Mech Min 42(1):109–125
van Genuchten MT (1980) A closed-form equation for predicting the hydraulic conductivity of unsaturated soils. Soil Sci Soc Am J 44(5):892–898